ISSN: 2710-0588

Hydrodynamic Analysis of Swept-wing Hydrofoils

Wei Ding[1], Zekai Sun[2], and Yangbing Liu[3]

[1] School of Navigation and Shipping, Shandong Jiaotong University, Weihai 264200, China

[2] China Merchants Jinling Shipyard (Yangzhou) Dingheng Co., Ltd, Yangzhou 225200, China

[3] Weihai Wuchuan Shipbuilding Co., Ltd, Weihai 264200, China

Abstract

This study aims to enhance the energy capture performance of oscillating hydrofoils for marine current and wave energy applications through geometric optimization. A straight hydrofoil is selected as the baseline, a swept leading-edge hydrofoil is used as the reference, and a kinked leading-edge modification is introduced. The computational domain and mesh refinement are constructed in ANSYS Workbench, and unsteady CFD simulations in Fluent are performed to evaluate lift, drag, moment power coefficient, and total power coefficient. Results indicate that the 15° swept hydrofoil improves lift and lift-to-drag ratio but reduces power output. Introducing a leading-edge kink modifies the near-field flow, strengthens pressure gradients and vortex structures, and ultimately increases both moment and total power coefficients beyond the baseline design. Vorticity and pressure analyses show that the kinked geometry delays flow separation and stabilizes power generation, offering guidance for marine energy converter design.

Keywords

Sweep-wing Hydrofoil, Hydrodynamics, Computational Fluid Dynamics (CFD).

1. Introduction

With the global energy system accelerating toward low-carbon and renewable development, ocean energy-characterized by strong predictability, large reserves, and high energy density-has attracted sustained attention as a strategic renewable resource for coastal and islanded power supply [1]. Among diverse conversion concepts, oscillating-hydrofoil harvesters utilize unsteady lift to extract energy from marine currents and waves, offering attractive engineering merits such as mechanical simplicity, adaptability in low-velocity flows, and reduced susceptibility to bio-fouling and entanglement [2–4]. For such devices, the formation, growth, and shedding of leading-edge vortices (LEVs) are widely recognized as the dominant flow mechanisms governing instantaneous lift response and cycle-averaged power output, making vortex regulation a central pathway for efficiency enhancement [5].

Recent advances in experimental diagnostics and high-fidelity numerical simulations have further highlighted that oscillating hydrofoils are intrinsically three-dimensional: spanwise flow, tip-vortex dynamics, and vortex–wake interactions can markedly alter load phasing and power stability across a cycle [6–8]. These findings motivate geometric and kinematic optimization strategies that aim to reshape near-field vortex topology, delay separation, and improve the moment–motion coupling responsible for energy capture [9]. In particular, leading-edge design plays a disproportionate role because it directly controls the onset and coherence of LEVs, thereby affecting the amplitude and temporal persistence of useful lift and pitching moment [10].

Despite these progresses, systematic understanding of how localized leading-edge discontinuities (e.g., kinked or broken leading edges) modify LEV evolution, moment generation, and the resulting power extraction under fully three-dimensional oscillatory

ISSN: 2710-0588

conditions remains limited [10–12]. Motivated by this gap, the present work adopts a straight hydrofoil as the baseline, introduces a swept leading edge as a reference, and further implements a kinked modification while keeping the same root and tip locations. Through fully three-dimensional unsteady CFD, the lift/drag/moment-based power and total power coefficients are quantified and correlated with vorticity and pressure fields, providing mechanistic guidance for high-efficiency oscillating-hydrofoil energy converters [10–12].

2. Description of the Oscillating Hydrofoil Problem

2.1. Energy-Extraction Mechanism of Oscillating Hydrofoils

Oscillating hydrofoils convert the kinetic energy of marine currents or waves into mechanical power through periodic unsteady lift generation. During the combined heaving–pitching motion, the hydrofoil experiences time-varying angles of attack that induce leading-edge vortex (LEV) formation, growth, and shedding within each cycle. These vortical structures enhance the instantaneous lift and generate oscillatory moments, forming the basis of energy extraction. The amplitude and phase of the lift response are strongly governed by the LEV strength, evolution rate, and detachment timing. As these characteristics depend sensitively on the hydrofoil's leading-edge geometry, geometric modification-such as introducing sweep or localized kinks-offers an effective strategy to regulate flow separation, manipulate spanwise flow, and improve the overall hydrodynamic performance of the device.

2.2. Kinematic Model of the Oscillating Hydrofoil

The commonly adopted motion form for oscillating hydrofoils consists of a combined trajectory in which the foil performs sinusoidal pitching about the pivot axis under incoming flow, superimposed with a heaving motion perpendicular to the flow direction, see Fig. 1.

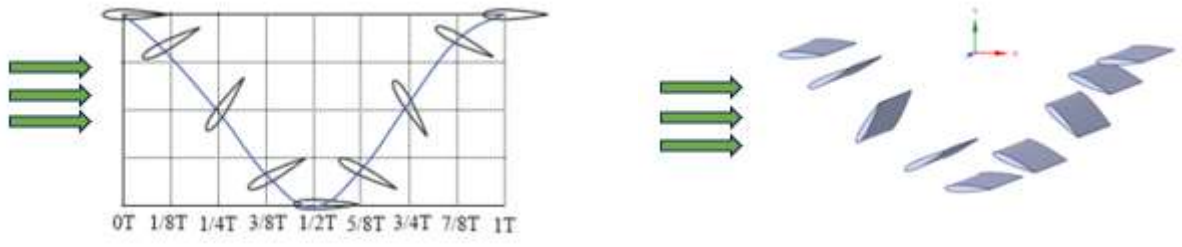

(a) Hydrofoil position at different times (b) Three-dimensional hydrofoil status

Fig. 1 Motion model of oscillating hydrofoil

The sinusoidal motion equation of the oscillating hydrofoil corresponding to the:

$$y(t) = -y_{\mathrm{m}} \sin(2\pi f t + \varphi). \tag{1}$$

$$\theta(t) = -\theta_{\mathrm{m}} \sin(2\pi f t). \tag{2}$$

In the above formula, f is the oscillation frequency, t is the current time, and φ is the heave pitch phase angle (defined as 90° in this study). The Reynolds number Re_c and the reduced frequency f^* are set as follows:

$$Re_c = U_\infty c/\nu. \tag{3}$$

ISSN: 2710-0588

$$f^* = fc / U_\infty . \tag{4}$$

In the above formula, U_∞ is the incoming flow velocity, ν is the fluid kinematic viscosity, and c is the hydrofoil chord length.

2.3. Hydrofoil Configurations and Geometric Characteristics

To systematically investigate the influence of leading-edge geometry on the unsteady hydrodynamic performance and energy-extraction capability of oscillating hydrofoils, three representative hydrofoil configurations are constructed and analyzed in the present study. Fig. 2 (a)–(c) illustrates the geometries of the straight leading-edge hydrofoil, the swept leading-edge hydrofoil, and the swept hydrofoil with a kinked leading edge, respectively. For all configurations, the root and tip locations, span length, and pitching-axis arrangement are kept identical to ensure that any observed differences in hydrodynamic response and power output arise solely from variations in leading-edge geometry.

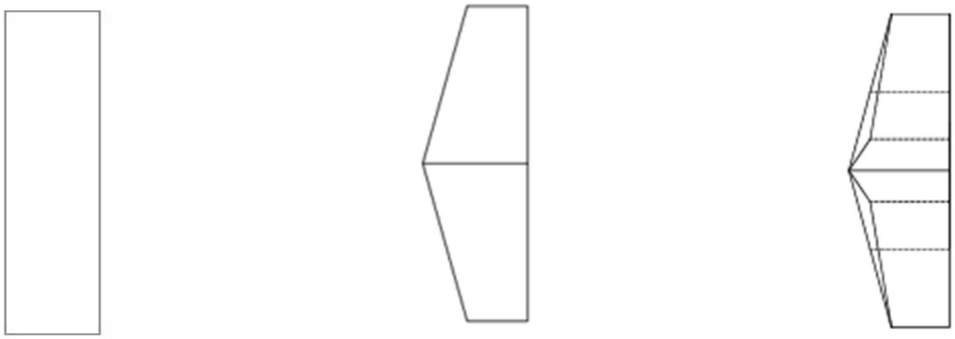

(a) Straight hydrofoil (b) Swept leading-edge hydrofoil (c) swept hydrofoil with a kinked leading edge.

Fig. 2 Swept oscillating hydrofoil

The straight leading-edge hydrofoil based on a standard NACA 0015 profile is adopted as the baseline configuration for performance comparison. On this basis, a uniform leading-edge sweep of 15° is introduced to modify the spanwise pressure gradient and vortex distribution, forming the swept leading-edge hydrofoil. Furthermore, a localized geometric kink is incorporated along the swept leading edge while maintaining unchanged root and tip positions, resulting in the kinked swept hydrofoil. This localized geometric discontinuity alters the effective planform area and leading-edge curvature distribution, thereby influencing flow separation characteristics, leading-edge vortex evolution, and unsteady moment generation. Through a comparative analysis of these three configurations, the effects of continuous geometric variation (sweep) and localized geometric modification (kink) on the energy-harvesting performance of oscillating hydrofoils can be systematically evaluated.

2.4. Governing Equations and Numerical Methods

The unsteady hydrodynamics of oscillating hydrofoils are solved by three-dimensional CFD simulations based on the incompressible Reynolds-averaged Navier–Stokes (RANS) equations. Turbulence effects are modeled using the Spalart–Allmaras (S-A) one-equation model, which has been widely applied to oscillating hydrofoil flows due to its robustness and computational efficiency in resolving boundary-layer development and mild flow separation. The governing equations are discretized using the finite volume method (FVM), with second-order accurate schemes adopted for both convective and diffusive fluxes. Time integration is performed using

ISSN: 2710-0588

a second-order implicit scheme, and pressure–velocity coupling is achieved via the PISO algorithm.

The prescribed hydrofoil motion consists of a superposition of vertical heaving and pitching about a fixed pivot axis, which is imposed through user-defined functions (UDFs). Both motions follow sinusoidal trajectories with fixed frequency and amplitude, ensuring fully controlled oscillatory kinematics. A uniform inflow velocity of 2 m/s is specified. Each simulation spans two complete oscillation periods and is discretized using 2000 time steps, corresponding to a time-step size of Δt = 0.000893 s, which provides sufficient temporal resolution to capture the generation, evolution, and shedding of leading-edge vortices.

The computational domain is subjected to a uniform velocity inlet and a pressure outlet, while slip-wall conditions are applied to the lateral and top boundaries. A no-slip condition is imposed on the hydrofoil surface. A hybrid structured–unstructured mesh is employed, with local refinement in the vicinity of the leading and trailing edges. Multiple layers of wall-adjacent cells are generated to ensure that the dimensionless wall distance satisfies $y+<1$, enabling accurate resolution of near-wall flow and vortex structures.

2.5. Governing Equations and Numerical Methods

The hydrodynamic forces and moments acting on the oscillating hydrofoil are obtained by integrating the pressure and viscous stresses over the hydrofoil surface at each time step. Based on the instantaneous force components in the streamwise and transverse directions, the lift force L, drag force D, and pitching moment M about the rotation axis are evaluated.

For consistent comparison among different hydrofoil configurations, the instantaneous hydrodynamic coefficients are expressed in nondimensional form as:

$$C_L = L/\frac{1}{2}\rho U_\infty^2 S. \tag{5}$$

$$C_D = D/\frac{1}{2}\rho U_\infty^2 S. \tag{6}$$

$$C_D = M/\frac{1}{2}\rho U_\infty^2 Sc. \tag{7}$$

Where ρ denotes the fluid density, U_∞ is the inflow velocity, c represents the hydrofoil chord length, and S represents the hydrofoil's frontal area. The instantaneous power P of the hydrofoil's captured energy is the sum of the work done by lift and the work done by pitching moment, where v is the hydrofoil's heave rate, and ω is the pitch rate.

$$P = L \cdot v + M \cdot \omega . \tag{8}$$

Therefore, the average power of the hydrofoil within one cycle is:

$$\bar{P} = \frac{1}{T}\int_0^T P\mathrm{d}t . \tag{9}$$

The total instantaneous power coefficient is then obtained as:

ISSN: 2710-0588

$$C_P = C_{PL} + C_{PM} = \frac{1}{U_\infty}[C_L v + C_M c\omega]. \tag{10}$$

For each case, the mean power coefficient is calculated by time-averaging the instantaneous power coefficient over one complete oscillation period after the flow reaches a periodic steady state. In addition, phase-averaged hydrodynamic coefficients are employed to examine the temporal evolution of force generation and energy extraction characteristics throughout the oscillation cycle.

3. Results and Flow-Field Analysis

This chapter presents the numerical results and flow-field analysis of three oscillating hydrofoil configurations, including the straight hydrofoil, the swept leading-edge hydrofoil, and the kinked swept leading-edge hydrofoil. The comparative assessment focuses on the time histories of hydrodynamic coefficients and power-related quantities, together with instantaneous vorticity fields, to elucidate the influence of leading-edge geometry on unsteady flow behavior and energy extraction mechanisms. Particular attention is paid to the formation, evolution, and shedding of leading-edge vortices, as well as their interaction with the hydrofoil motion. By correlating vortex dynamics with force and moment responses, the role of localized geometric modification in regulating flow separation and enhancing power-related performance is systematically examined, providing physical insight into the performance improvement observed in the modified hydrofoil configuration.

3.1. Time-Resolved Hydrodynamic Response

Fig. 3 presents the time histories of the lift coefficient C_L, drag coefficient C_D, moment power coefficient C_{PM}, and instantaneous power coefficient C_P for the straight hydrofoil (SH), swept leading-edge hydrofoil (SLH), and kinked swept leading-edge hydrofoil (K-SLH) over one complete oscillation cycle. All simulations are conducted under identical inflow and kinematic conditions to ensure a consistent comparison among different leading-edge configurations.

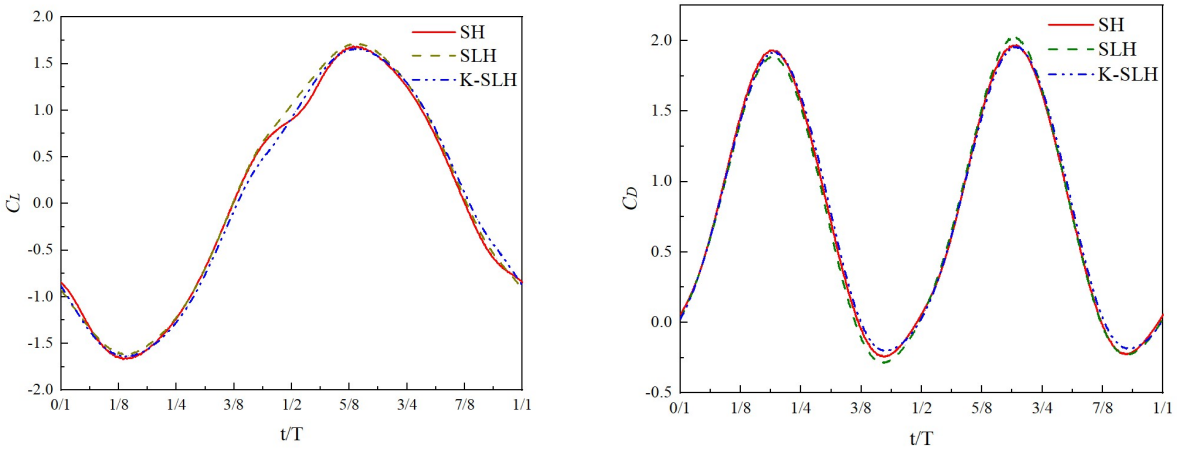

(a) lift coefficient C_L (b) drag coefficient C_D

ISSN: 2710-0588

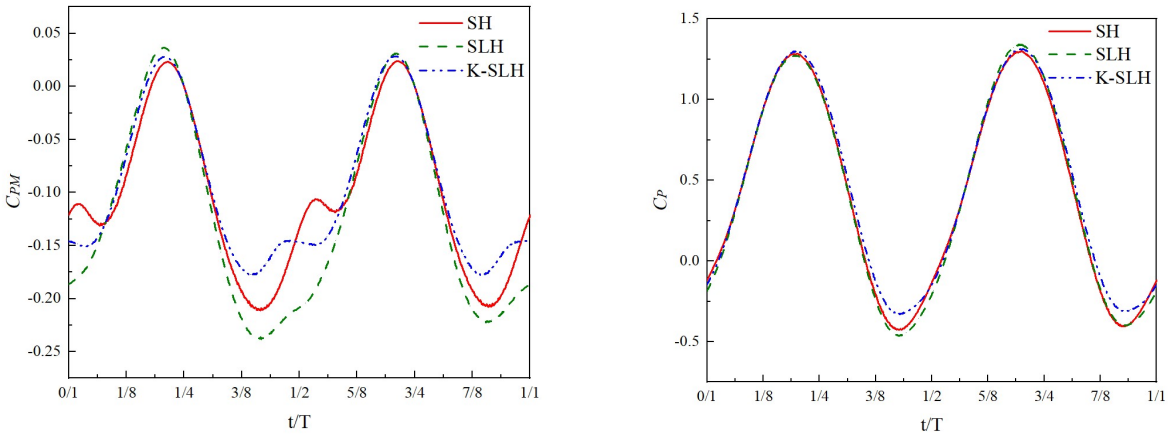

(c) moment power coefficient C_{PM} (d) instantaneous power coefficient C_P

Fig. 3 Time histories of hydrodynamic and power coefficients over one oscillation cycle

As shown in Figs. 3(a) and (b), all three hydrofoil configurations exhibit clear periodic behavior in both lift and drag coefficients, indicating that the oscillatory motion has reached a stable limit-cycle state. Compared with the straight hydrofoil, the swept leading-edge hydrofoil produces slightly higher lift peaks, reflecting the enhancement of unsteady lift induced by the leading-edge sweep. In contrast, the kinked swept hydrofoil shows smoother lift variations with a marginally reduced peak value, while the amplitude of drag fluctuations is noticeably suppressed. This behavior suggests that the localized geometric discontinuity moderates flow separation and reattachment processes during the oscillation cycle.

More pronounced differences among the three configurations are observed in the moment power coefficient C_{PM}, as shown in Fig. 3(c). The straight hydrofoil exhibits significant negative power intervals during the oscillation, whereas the swept hydrofoil shows even deeper negative peaks, indicating an unfavorable phase relationship between the hydrodynamic moment and pitching motion. By comparison, the kinked swept hydrofoil generates higher and more sustained positive moment power, with substantially reduced negative power regions throughout the cycle.

The instantaneous power coefficient C_P shown in Fig.3(d) further confirms these trends. The straight and uniformly swept hydrofoils experience large temporal fluctuations and extended negative power intervals, whereas the kinked swept hydrofoil maintains a higher instantaneous power level over most phases of the oscillation. Moreover, its power output exhibits improved temporal smoothness, indicating enhanced stability of energy extraction. These results demonstrate that while a swept leading edge alone improves lift characteristics, it does not necessarily lead to higher power output. Introducing a leading-edge kink effectively regulates the coupling between unsteady hydrodynamic loads and oscillatory motion, resulting in a marked improvement in power extraction performance.

3.2. Phase-resolved Vortex Dynamics

As indicated by the time histories of the power-related coefficients, one oscillation cycle of the three hydrofoils can be divided into a dominant positive-power stage, a rapid decay stage, and a negative-power stage. To clarify how the leading-edge geometry affects the flow structures in these stages, three representative instants, t/T=0.25, 0.375 and 0.5, are selected for flow-field analysis. The first instant corresponds to the vicinity of the main peak of the instantaneous power coefficient C_P, the second lies on the descending branch as the power starts to decrease, and the third is located within the negative-power interval. The spanwise vorticity fields of the

ISSN: 2710-0588

three oscillating hydrofoils at these instants are examined using iso-surfaces of Z-vorticity, where the color scale denotes the magnitude and sign of the vorticity, see Fig. 4.

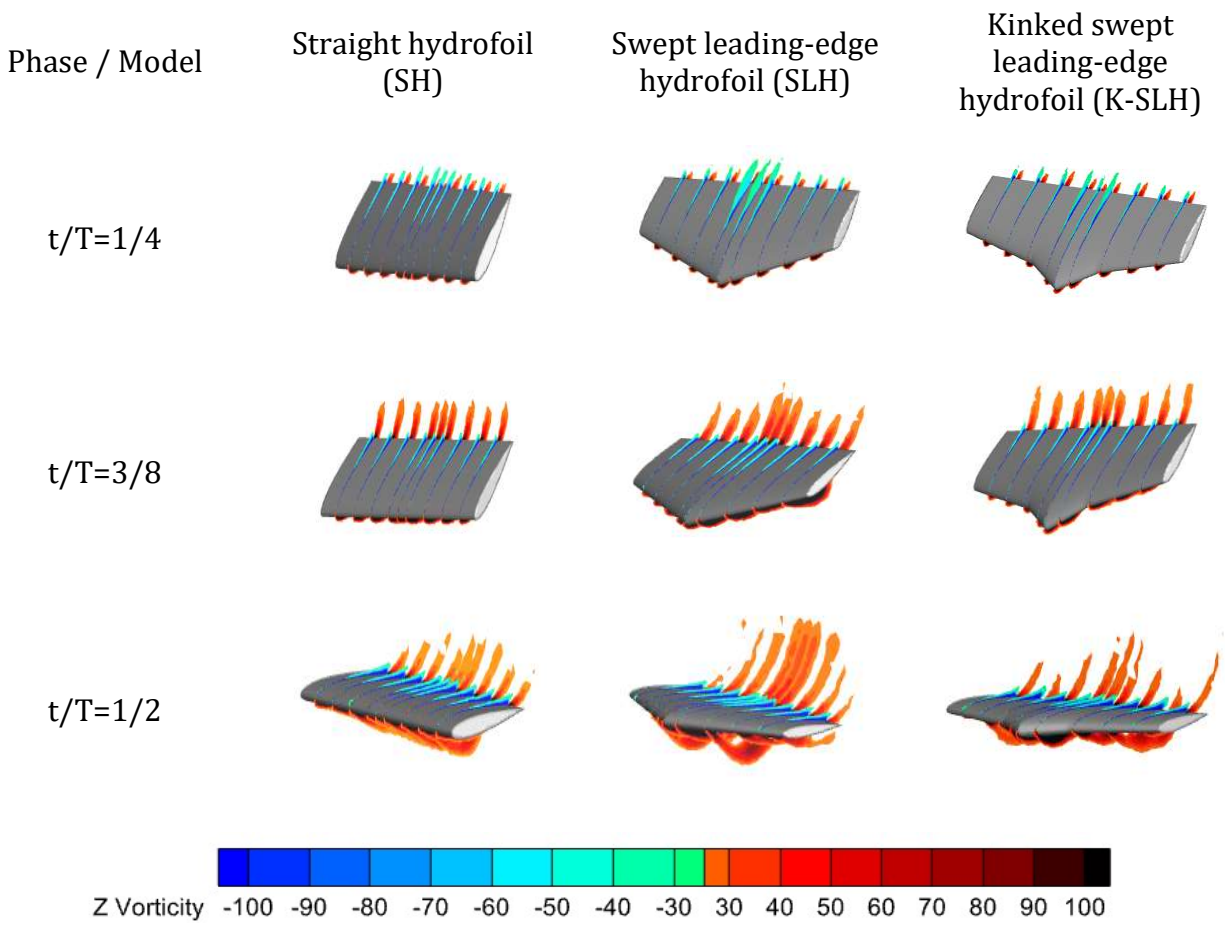

Fig. 4 Vorticity contours of different hydrofoil configurations at selected oscillation phases

At t/T=0.25, all configurations generate a leading-edge vortex (LEV) over the suction side that is closely associated with the positive power output. For the straight hydrofoil, the LEV is relatively short and of moderate strength, with the core concentrated near the mid-span. Introducing uniform sweep elongates the LEV in the spanwise direction and enhances vorticity transport from root to tip; however, the vortex core moves farther away from the suction surface and begins to break up near the tip, which limits its beneficial contribution to lift. In contrast, the kinked swept hydrofoil develops a stronger and more coherent LEV that remains attached over a wider spanwise extent. The kink modifies the distribution of spanwise vorticity, causing thicker vortex tubes on both sides of the kink and substantially increasing the local suction. As a result, this configuration can sustain a high level of instantaneous power over a longer portion of the positive-power stage.

At t/T=0.375, corresponding to the transition between the positive- and negative-power stages, the LEV on the straight and uniformly swept hydrofoils has already started to detach from the suction surface, and the near wake is dominated by fragmented, highly three-dimensional vortices convecting downstream. This early shedding is accompanied by a rapid decrease in C_P and deep negative values of C_{PM} . By contrast, the kinked swept hydrofoil still exhibits a relatively compact LEV core that remains partially attached near mid-span; the alignment of vortex tubes in the spanwise direction is better preserved, and the wake appears less disordered.

ISSN: 2710-0588

At t/T=0.5, within the negative-power stage, large-scale reverse-flow vortices appear near the suction side and in the wake of the straight and uniformly swept hydrofoils, inducing strong adverse pitching moments and leading to substantial negative power. For the kinked swept hydrofoil, the reverse vortical structures are noticeably weaker and more diffuse, and the vorticity distribution is smoother without severe vortex breakdown in the wake. The attenuation of unsteady vortex breakdown not only reduces the magnitude of instantaneous negative power but also shortens its effective duration. Consequently, the kinked swept configuration achieves a higher cycle-averaged power coefficient and improved temporal stability of power output. This phase-resolved analysis of vortex dynamics provides direct flow-field evidence of the flow-control benefits offered by the kinked leading edge in oscillating-hydrofoil energy harvesters.

4. Conclusion

This study conducted three-dimensional unsteady CFD simulations of three oscillating hydrofoil configurations-a straight leading edge, a uniformly swept leading edge, and a kinked swept leading edge-under identical kinematic conditions. The results demonstrate that leading-edge geometry exerts a primary influence on unsteady hydrodynamic loads and energy-harvesting performance. Introducing uniform sweep slightly enhances peak lift and the lift-to-drag ratio but intensifies negative moment power and prolongs negative-power intervals, yielding no net improvement in the cycle-averaged power coefficient.

By contrast, incorporating a localized kink along the swept leading edge substantially reorganizes the three-dimensional vortex system. At t/T=0.25, the kinked configuration promotes the formation of a stronger, spanwise-coherent leading-edge vortex that supports the peak positive power output. At t/T=0.375, it delays vortex shedding and maintains a more ordered wake, thereby slowing the decay of instantaneous power. At t/T=0.50, it attenuates reverse-flow vortices and mitigates adverse power contributions. Consequently, the kinked swept hydrofoil achieves higher and more sustained positive power, reduced negative power, and a significantly increased mean power coefficient, while preserving the same root–tip layout and global motion parameters. These findings indicate that simple, localized leading-edge discontinuities provide an effective passive flow-control strategy for oscillating-hydrofoil energy harvesters and offer practical guidance for the geometric optimization of marine current and wave energy converters.

References

[1] Information on https://www.etipocean.eu/knowledge_hub/1687/

[2] A. B. Kinsey and G. Dumas: Parametric Study of an Oscillating Airfoil in Power-Extraction Mode, Journal of Fluids and Structures, Vol. 32 (2012), p. 1-20.

[3] Y. Zhang, X. Wang and J. Liu: Energy Harnessing Performance of Oscillating Foil Submerged in the Wake of a Circular Cylinder, Energies, Vol. 17 (2024) No. 8, p.1793.

[4] J. X. Xiao and Q. Zhu: A Review on Flow Energy Harvesters Based on Flapping Foils, Journal of Fluids and Structures, Vol. 46 (2014), p. 174-191.

[5] G. Bräuninger: Proc. International Workshop on Diamond Tool Production (Turin, Italy, November 8-10, 1999). Vol. 1, p.154.

[6] H. Qu, Y. Zhao and Z. Li: Semi-Passive Energy Extraction of a Coupled-Pitching Hydrofoil under Semi-Passive Mode, Applied Ocean Research, Vol. 163 (2025), p.104585.

[7] J. Wang, Y. Sun and M. Chen: Numerical Investigation on Three-Dimensional Effects of Oscillating Hydrofoils for Marine Current Energy Harvesting, Ocean Engineering, Vol. 295 (2024), p. 1-15.

ISSN: 2710-0588

[8] M. Hasanvand, A. E. Bakhshandeh and H. Ghassemi: Performance Enhancement of Tandem Oscillating Hydrofoils for Hydrokinetic Energy Harvesting, Renewable Energy, Vol. 180 (2021), p. 1-18.

[9] Y. Sun, K. He and Z. Zhang: Hydrodynamic Response and Vortex Evolution of an Oscillating Hydrofoil under Complex Oscillation Modes, Physics of Fluids, Vol. 34 (2022) No. 5, p. 1-15.

[10] T. McKinney and J. DeLaurier: The Wingmill: An Oscillating-Wing Windmill, AIAA Journal, Vol. 19 (1981) No. 12, p. 1-10.

[11] J. Read, M. S. Triantafyllou and F. S. Hover: Forces on Oscillating Foils for Propulsion and Maneuvering, Journal of Fluids and Structures, Vol. 17 (2003) No. 1, p. 163-183.

[12] J. Young and J. C. S. Lai: Mechanisms Influencing the Efficiency of Oscillating-Foil Energy Harvesters, Journal of Fluids and Structures, Vol. 23 (2007) No. 5, p. 1-16.